Published in final edited form as:
Environ Sci Technol. 2013 November 5; 47(21): . doi:10.1021/es402838f.

Stereoselective Formation of Mono- and Di-Hydroxylated Polychlorinated Biphenyls by Rat Cytochrome P450 2B1

Zhe Lu[#1], **Izabela Kania-Korwel**[#2], **Hans-Joachim Lehmler**[2,*], and **Charles S. Wong**[1,3,*]

[1]Department of Chemistry, University of Manitoba, Winnipeg, MB, R3T 2N2, Canada

[2]Department of Occupational and Environmental Health, College of Public Health, University of Iowa, Iowa City, Iowa 52242,United States

[3]Department of Environmental Studies and Sciences and Department of Chemistry, Richardson College for the Environment, University of Winnipeg, Winnipeg, MB, R3B 2E9, Canada.

[#] These authors contributed equally to this work.

Abstract

Changes in atropisomer composition of chiral polychlorinated biphenyls (PCBs) and their mono- and di- hydroxylated metabolites (OH- and diOH-PCBs) via rat cytochrome P450 2B1 (CYP2B1) mediated biotransformation were investigated *in vitro*. Rat CYP2B1 could stereoselectively biotransform chiral PCBs to generate *meta*-OH-PCBs as the major metabolites after 60 min incubations. Non-racemic enantiomer fractions (EFs: concentration ratios of the (+)-atropisomer or the first-eluting atropisomer over the total concentrations of two atropisomers) of 5-OH-PCBs, were 0.17, 0.20, 0.85, 0.77 and 0.41 for incubations with PCBs 91, 95, 132, 136 and 149, respectively. CYP-mediated stereoselective formation of diOH-PCBs from OH-PCBs was observed for the first time. After 60 min stereoselective biotransformation, the EFs of both 4-OH-PCB 95 and 5-OH-PCB 95 changed from racemic (i.e., 0.50) to 0.62 and 0.46, respectively. These transformations generated statistically non-racemic 4,5-diOH-PCB 95, with EFs of 0.53 and 0.58 for 4-OH-PCB 95 and 5-OH-PCB 95 incubations, respectively. Biotransformation of PCBs 91 and 136 also generated 4,5-diOH-PCB 91 and 4,5-diOH-PCB 136, respectively. These *in vitro* results were consistent with that observed for stereoselective PCB biotransformation by rat liver microsomes and *in vivo*. Biotransformation interference between two atropisomers of PCB 136 was investigated for the first time in this study. The biotransformation process of (−)-PCB 136 was significantly disrupted by the presence of (+)-PCB 136, but not the other way around. Thus, stereoselective metabolism of chiral PCBs and OH-PCBs by CYPs is a major mechanism for atropisomer composition change of PCBs and their metabolites in the environment, with the degree of composition change dependent, at least in part, on stereoselective interference of atropisomers with each other at the enzyme level.

INTRODUCTION

Non-racemic atropisomer distribution of chiral polychlorinated biphenyls (PCBs) have been detected in many biota, both in the wild and the laboratory.[1-2] Differential accumulation of the individual atropisomers of chiral PCBs in biota (species-specific, organ-specific and congener-specific) indicates that they are subject to different stereoselective metabolic processes, toxicities and fate in the biosphere. For example, the activation of ryanodine receptors and other cellular targets, and consequent disruption of Ca^{2+} signaling by chiral

[*]Corresponding authors: Lehmler--Phone: +1-319-335-4310; Fax: +1-319-335-4290; hans-joachim-lehmler@uiowa.edu Wong--Phone: +1-204-786-9335; Fax: +1-204-775-2114; wong.charles.shiu@alum.mit.edu.

PCBs, are stereoselective processes in organisms and thus different atropisomers may cause different neurotoxicities.[3-6]

Stereoselective biotransformation by cytochrome P450 isozymes (CYPs) is a major mechanism for the atropisomer composition change of chiral PCBs in biota.[7-9] PCBs are oxidized by CYPs to generate PCB arene oxide intermediates and/or OH-PCBs, the former of which can be converted to OH-PCBs by epoxide hydroxylase.[10] However, the individual stereoisomers of a chiral chemical can bind to CYPs with different affinities and thus have different biotransformation kinetics, which can be affected by the presence of other xenobiotics or endogenous chemicals.[9] Therefore, it is plausible that the two atropisomers of a chiral PCB could disrupt the enzymatic biotransformation processes of each other, as previously observed for (+)- and (−)-PCB 132 with rat CYP2B1.[9] However, unanswered questions still remain due to limitations of these earlier studies, including low purity and/or concentration of CYPs and enantiopure PCB atropisomers, short incubation times and lack of analysis of metabolites.[9, 11]

OH-PCBs have been found in many species *in vitro* or *in vivo*.[12-19] These metabolites are also of environmental concern because they can result in dysfunction of thyroid and estrogenic activities,[10] disruption of the homoeostasis of vitamin A,[20] disorder in neuronal and brain development,[21] cytotoxicity and oxidative stress in cells,[22] and interference with the metabolism of xenobiotics in other organisms.[23] Atropisomer accumulation of OH-PCBs in biota may also result in stereoselective toxicities.

Previous studies[8,24,25] found that 5-OH-PCBs were formed stereoselectively as the major metabolites of chiral PCBs by rat liver microsomes and tissue slices. Atropisomer enrichment of OH-PCB 136 and the formation of diOH-PCBs in the livers of rats and mice were also observed *in vivo*.[26, 27] *In vitro*, rat CYP2B1 could biotransform chiral PCBs stereoselectively to form OH-PCB metabolites.[7] However, specific metabolites could not be identified due to lack of standards[7], nor were the EFs of OH-PCBs determined. Thus, although it is reasonable to presume that CYPs are the major enzymes responsible for stereoselective formation of OH-PCBs in animals, specific pathways for stereoselective biotransformation of PCBs to form specific OH-PCBs remain unclear. In addition, diOH-PCBs were also detected in some organisms as metabolites of PCBs.[28-30] These metabolites can be formed through hydroxylation of OH-PCBs[31] by CYP2B1[32] in rat liver microsomes.[31, 33] However, the stereoselectivities of this hydroxylation of OH-PCBs and the formation of diOH-PCBs by purified CYPs are unknown.

In the present study, we address the questions raised above by the previous studies. Rat CYP2B1 was used in our experiment because it could stereoselectively biotransform chiral PCBs.[7] We hypothesized that 5-OH-PCB was the major metabolite of chiral PCB by rat CYP2B1 biotransformation and the formation of OH-PCB was a stereoselective process; that 4-OH-PCB and diOH-PCB metabolites could also be formed in this biotransformation process as minor products; and that chiral OH-PCBs could be stereoselectively biotransformed by rat CYP2B1 to produce non-racemic diOH-PCBs. In addition, we also hypothesized that an increase in concentration of one atropisomer will decrease the biotransformation activity of its antipode, and that disruption in biotransformation activity when both atropisomers are present to varying degrees, stereoselectively or otherwise, will affect the formation of hydroxylated metabolites. To our knowledge, this is the first time that purified CYP isozymes are shown to produce OH-PCBs stereoselectively, which in turn are stereoselectively metabolized to diOH-PCBs.

EXPERIMENTAL SECTION

Chemicals and Regents

Racemic 2,2',3,4',6-pentachlorobiphenyl (PCB 91), 2,2',3,5',6-pentachlorobiphenyl (PCB 95), 2,2',3,3',4,6'-hexachlorobiphenyl (PCB 132), 2,2',3,3',6,6'-hexachlorobiphenyl (PCB 136), 2,2',3,4',5',6-hexachlorobiphenyl (PCB 149), surrogate standards 2,4,6-trichlorobiphenyl (PCB 30), 2,2',3,4,4',5,6,6'-octachlorobiphenyl (PCB 204) and 2',3,3',4', 5,5'-hexachlorobiphenyl-4-ol (4-159), and internal standards 2,3,4',5,6-pentachlorobiphenyl (PCB 117) and 2,3,3',4,5,5'-hexachlorobiphenyl (PCB159) (all purities >99%) were purchased from Accustandard (West Haven, CT) and stock solutions were prepared in acetone. Rat CYP2B1 (CYP2B1 itself+CYP reductase+cytochrome b_5), insect cell control supersomes (CYP reductase+cytochrome b_5) (stored at −80°C until use) and NADPH regeneration system (solution A: 31 mM $NADP^+$, 66 mM glucose-6-phosphate and 66 mM $MgCl_2$ in water; solution B: 40 U/ml glucose-6-phosphate dehydrogenase in 5 mM sodium citrate) (stored at −20°C until use) were purchased from BD Biosciences (San Jose, CA).

Individual PCB 136 atropisomers were isolated as previously published.[11] The following authentic PCB metabolite standards were synthesized as described previously:[11,32] 3-methoxy-2,2',4,4',6-pentachlorobiphenyl (3-100, NIH-shift metabolite of PCB 91); 2,2',3,4', 6-pentachlorobiphenyl-4-ol (4-91); 2,2',3,4',6-pentachlorobiphenyl-5-ol (5-91); 3,4-dimethoxy-2,2',4',5,6-pentachlorobiphenyl; 3-methoxy-2,2',4,5',6-pentachlorobiphenyl (3-103, NIH-shift metabolite of PCB 95); 2,2',3,5',6-pentachlorobiphenyl-4-ol (4-95); 4-methoxy-2,2',3',5,6'-pentachlorobiphenyl (4'-95); 2,2',3,5',6-pentachlorobiphenyl-5-ol (5-95); 3,4-dimethoxy-2,2',5,5',6-pentachlorobiphenyl; 3-methoxy-2,2',3',4,4',6-hexachlorobiphenyl (3'-140); 2,2',3,3',4',6-hexachlorobiphenyl-4-ol (4'-132); 2,2',3,3',4',6-hexachlorobiphenyl-5-ol (5'-132); 3,4-dimethoxy-2,2',3',4',5,6-hexachlorobiphenyl; 2,2',3', 4,6,6'-hexachlorobiphenyl-3-ol (3'-150); 2,2',3,3',6,6'-hexachlorobiphenyl-4-ol (4-136); 2,2', 3,3',6,6'-hexachlorobiphenyl-5-ol (5-136); 3,4-dimethoxy-2,2',3',5,6,6'-hexachlorobiphenyl; 3-methoxy-2,2',4,4',5',6-hexachlorobiphenyl (3'-154); 2,2',4',5,5',6-hexachlorobiphenyl-3-ol (5-149). Standard solutions were prepared in isooctane for methoxy-compounds and in methanol for hydroxy-compounds.

The following abbreviations are used for diOH-PCBs: 4,5-91, 4,5-95, 4'5'-132 and 4,5-136 for 3,4-dihydroxy-2,2',4',5,6-pentachlorobiphenyl, 3,4-dihydroxy −2,2',5,5',6-pentachlorobiphenyl, 3,4-dihydroxy-2,2',3',4',5,6-hexachlorobiphenyl and 3,4-dihydroxy −2,2',3',5,6,6'-hexachlorobiphenyl, respectively.

In vitro biotransformation experiments

Details on incubation methods were previously published.[7,9] Briefly, incubations were conducted in glass tubes containing 10 pmol of rat CYP2B1, 50 μL of solution A, 10 μL of solution B, 1000 ng PCB or OH-PCB, and potassium phosphate buffer (110 mM, pH 7.4) in 1 mL total volume at 37°C for 60 minutes. Incubations were intended to generate enough products for enantioselective analyses. Hence, relatively high concentrations (1000 ng/mL) of PCBs or OH-PCBs were used, and enzymatic biotransformation activities may not necessarily be linear over the entire period of the incubation as previously observed[9]. Incubations were terminated with 1 mL ice-cold methanol and immediately extracted. PCB 95 was used as a positive control substrate for 60 minute incubations. Different chiral PCBs were incubated with CYP control supersomes instead of rat CYP2B1 for 60 minutes as negative controls. Incubations were done in triplicate except for the control samples.

To understand better how the stereoisomers of a chiral contaminant may interfere with their enzymatic biotransformation, individual atropisomers of PCB 136 were isolated and used in the biotransformation experiment. We added the same concentration (500 ng/mL) of one

atropisomer of PCB 136, i.e., (+)-PCB 136 or (−)-PCB 136, in the incubations and then varied the concentration (0, 100, 250, or 500 ng/mL) of its antipode i.e., (−)-PCB 136 or (+)-PCB 136 in that incubation. Please see the Support Information (SI) for more details.

Chemical extraction and clean-up

Extraction methods are also detailed elsewhere.[7,9] Briefly, PCBs 30, 204 and 4-OH-PCB 159 were added as surrogate standards after the incubations were terminated to the test tubes. The incubations were further denatured using HCl and 2-propanol, vortexed for 1 min and centrifuged for 10 min. The liquid supernatant was then washed with KCl and extracted with 6 mL of 1:1 (v/v) methyl-*t*-butyl ether (MTBE)/hexane. The organic phase was collected and partitioned with 6 mL of 1:1 (v/v) 1 M KOH/ethanol to separate the OH-PCBs from the neutral organic phase. PCBs in the neutral organic fraction were purified using an acidified silica gel column (3 g, 22% H_2SO_4) and eluted with 20 mL of 15% (v/v) dichloromethane/hexane. PCB fractions were solvent-exchanged to hexane, and PCB 159 was added as an internal standard. OH-PCBs in the aqueous fraction were then acidified by H_2SO_4 and back-extracted into MTBE/hexane (1:1, v/v). The organic phase containing OH-PCBs was derivatized with diazomethane into their respective methoxy-PCBs (MeO-PCBs). The MeO-PCB fraction was purified using a 5 g column of the acidified silica gel and eluted with 50 mL of 1:1 (v/v) dichloromethane/hexane. MeO-PCB fractions were solvent-exchanged to hexane and PCB 117 was added as an internal standard. Every extraction step was repeated three times for each sample.

The average and standard deviations of PCBs 30 and 204 recoveries were 91±17% and 79±9% respectively, and PCB concentrations were corrected based on the average recoveries of PCBs 30 and 204 in each sample. Likewise, the recovery of 4-OH-PCB 159 was 82±22%. MeO-PCB concentrations were corrected by the recovery of 4-OH-PCB 159 in each sample except for PCB 132 which had co-elution issues.[27] PCB concentrations were determined using PeakFit v4.12 (Systat Software, San Jose, CA) to deconvolute chromatographic peaks and maintain consistentency with previous studies.[9, 34] For the same reason, integration of Meo-PCB peaks were performed using the valley-drop method.[8]

Instrumentation and measurements

PCBs were quantified using an Agilent 5890 gas chromatograph with a ^{63}Ni-μ electron capture detector (ECD) and a Chirasil-Dex (CD) column (25 m×0.25 mm internal diameter (i.d.)×0.25 μm d_f, Agilent, Santa Clara, CA).[7, 9] One μL samples were injected in the splitless mode at 250 °C with helium as carrier gas and at a constant column head pressure of 0.71 bar. Initial oven temperature was held at 60°C for 2 min, then ramped at 10°C/min to 160°C, ramped at 1°C/min to 210°C, held for 25 min. The detector temperature was 320°C.

MeO-PCB congeners were quantified using an Agilent 7890A gas chromatograph with a ^{63}Ni-μECD detector and SPB-1 or Equity-1 column (60 m×0.25 mm i.d.×0.25 μm d_f, respectively; Supelco, St. Louis, MO). The following temperature program was used: 150°C for 2 min, then 30°C/min to 200°C, 1°C/min to 230°C, 10°C/min to 300°C, hold for 15 min, with the constant helium flow of 2 mL/min. The injector and detector temperatures were 280°C and 300°C, respectively.[27]

The identity of hydroxylated metabolites, as their methoxylated derivatives, was confirmed on an Agilent 7890A gas chromatograph with a 5975C mass spectrometry detector and a HP-5 column (30 m×0.32 mm i.d.×0.25 μm d_f, Agilent, Santa Clara, CA). The following temperature program was used: 100°C for 1 min, then 5°C/min to 280°C with the constant helium flow of 1.5 mL/min. The ions monitored were *m/z* 356 and 358 for mono-methoxylated pentachlorobiphenyls, *m/z* 384 and 386 for di-methoxylated

pentachlorobiphenyls, *m/z* 390 and 392 for mono-methoxylated hexachlorobiphenyls, and *m/z* 420 for di-methoxylated hexachlorobiphenyls. The injector, source and quadrupole temperatures were 280°C, 230°C and 180°C, respectively.[27]

To facilitate the enantioselective analysis, EF determinations of MeO-PCBs were performed using an Agilent 7890A gas chromatograph equipped with two ^{63}Ni-μECD detectors, a CD column (30 m×0.25 mm i.d.×0.39 μm d_f) and a ChiralDex B-DM (BDM) column (30 m×0.25 mm i.d.×0.12 μm d_f; Supelco, St. Louis, MO). Two columns were used to help confirm enantiomeric composition, both of which could resolve all MeO-PCB congeners studied. The following temperature program was used: 100°C for 1 min, 10°C/min to 140°C, hold for 460 min, 1°C/min to 200°C, hold for 35 min with the constant helium flow of 3 mL/min. The injector and detector temperatures were held at 250°C. For incubation samples containing PCB 132 and its metabolites, the final temperature was 160°C to optimize isomer/atropisomer separation.[8]

Data Analyses

The enantiomer fraction (EF) was defined as EF=E(+)/(E(+)+E(−)), where the elution order of (+) and (−) atropisomer is known (PCBs 132, 136 and 149),[35,36] or EF=E1/(E1+E2) where the elution order is unknown. Prism 5 (GraphPad Software, La Jolla, CA) was used for plotting and statistical analyses. The *t*-test and one way ANOVA were used for data analyses, with statistically significant levels at 0.05 (please see figure captions for details).

RESULTS AND DISCUSSION

Stereoselective biotransformation of chiral PCBs

PCBs 91, 95, 132, 136 and 149 were chosen as substrates because they are widely detected in organisms as non-racemic residues[37, 38] and are neurotoxic.[3-6] Depletions of PCBs 91, 95, 132, 136 and 149 were 25%, 17%, 11%, 21% and 4% after 60 min incubation, respectively. PCBs 91 and 95 were biotransformed more rapidly than PCBs 132 and 149, but similar with PCB 136 (Fig. 1A1). It is well-established that the biotransformation rate of PCBs depends on the presence of unsubstituted vicinal *meta* and *para* positions,[10] as well as substrate sizes,[39] binding positions and affinities to enzymes.[9] All these congeners, except for PCB 149, were stereoselectively biotransformed by rat CYP2B1 (Fig. 1A1 and 1A2). The biotransformation activities of E1-91, E2-95, (−)-132 and (+)-136 were significantly higher than their respective antipodes (Fig. 1A1). Accordingly, the EFs of PCBs 91, 95, 132 and 136 changed from the racemic value (i.e., 0.50) to 0.45 (not statistically different), 0.57, 0.55 and 0.47, respectively. In contrast, PCB 149 was slightly biotransformed by rat CYP2B1, but with no apparent stereoselectivity (Fig. 1A1). All atropisomer composition patterns observed in the present work were consistent with previous rat CYP2B1-mediated *in vitro* experiments.[7, 9] One possible mechanism for the stereoselective biotransformation at the molecular level is that the binding orientation and affinities of two atropisomers with a specific enzyme are not exactly the same.[9] Consequently, these interaction differences could result in different biotransformation kinetics of the two atropisomers of a congener.

Likewise, the atropisomer composition patterns of PCBs 91, 95, 132 and 136 observed in the present study (Fig. 1A2) were consistent with previous rat liver microsomal experiments. For example, the EFs of PCBs 91, 95, 132 and 136 after 30 min microsomal incubations were 0.43, 0.64, 0.61 and 0.40 respectively,[8, 24] which were similar to our observations (Fig. 1A2). The slight differences in EFs observed between the present study and previous literature might be due to differences in initial substrate concentrations, rat CYP2B1 content, involvement of other CYPs in microsome incubation, incubation time, and chromatographic integration methods.[7, 9, 34] Taken together, all these observations demonstrate that CYP2B1

is one of the enzymes responsible for the stereoselective biotransformation of these chiral PCB congeners in rat liver. However, PCB 149 after 30 min biotransformation by rat liver microsomes was significantly non-racemic with an EF of 0.46,[8] in contrast to our observation of no significant atropisomer composition change in the present study. This difference in atropisomer composition pattern of PCB 149 suggests that CYPs other than CYP2B1 in the liver microsomes might have been involved. Phase II biotransformation was unlikely to affect stereoselectivity in that case, because cytosolic phase II enzymes and co-factors of cytosolic and microsomal phase II enzymes are removed during the preparation of microsomes by differential centrifugation.

Stereoselective biotransformation of chiral PCBs by different types of enzymes might be one of the major reasons for the tissue-, species- and congener-specific atropisomer accumulation observations *in vivo*. The atropisomer composition signatures of PCBs 95 and 132 measured in this study were consistent with the previous *in vivo* observations for rats (EFs>0.5),[40, 41] suggesting that CYP2B1 mediated biotransformation might be one reason for the atropisomer composition change of these congeners in rats. Similar EFs of PCB 95 were also detected in thick-billed murre, ivory gull, ringed seal,[37] and harbour porpoises,[38] indicating that CYP 2B1-like enzymes mediated biotransformation might be involved in these high tropic level species. However, different composition patterns of chiral PCBs were observed in some species. The EFs of PCBs 95 and 136 were about 0.3 and 0.7, respectively, in C57Bl/6 female mice tissues after oral administration.[26, 42] These results indicate that, besides CYP-mediated biotransformation, other processes (e.g. induction of CYP-enzymes by drugs or environmental contaminants,[24, 25] modulation of CYP activity by other chemicals (e.g., gold nanoparticles),[43] phase II metabolism, or active transport processes) cannot be excluded as factors contributing to the atropisomer composition changes of PCBs *in vivo*.

Stereoselective formation of hydroxylated PCBs

Hydroxylated metabolites were detected in the incubations of parent PCB congeners, dominated by *meta*-substitution into the 2,3,6-trichlorinated ring to generate 5-OH-PCBs (or 5'-OH-PCB for PCB 132) (Fig. 1B1 and Fig. S1). The unsubstituted vicinal *meta* and *para* positions of 2,3,6-substituted PCBs make them amenable to oxidation by CYP2B isozymes.[39] The yields, expressed as the percent of 5-OH-PCB over the initial PCB amount in the incubation, of 5-OH-PCBs were 5.4%, 12%, 5.9%, 19%, 1.6% for PCBs 91, 95, 132, 136 and 149, respectively. In addition, 4-OH-PCB metabolites were detected by GC-ECD analysis as minor products from incubations of PCBs 91, 95 and 136. The formation of these metabolites could not be confirmed by GC-MS due to the low levels of these metabolites in the incubations.

After 60 min, approximately 22%, 71%, 53%, 90%, and 46% of PCBs 91, 95, 132, 136 and 149 of the depleted PCBs were converted to the corresponding 5-OH-PCBs metabolites, respectively. In contrast, relatively lower amounts of the observed depletion of PCBs 91 (less than 1%), 95 (about 25%) and 136 (less than 5%) were converted to their 4-hydroxylated and 4,5-dihydroxylated metabolites. This rough mass balance calculation suggests that the remaining fraction of the parent PCBs might have been biotransformed to currently unidentified metabolites, including other OH-PCB or arene oxide metabolites. Indeed, some unidentified peaks were observed in the chromatograms (e.g., metabolites of PCB 95, Fig. S1B), which was consistent with previous observations in rat liver microsomes.[8] We could not identify the arene oxide intermediates in the present study because the experiment was not designed for collecting these intermediates.

The formation of 5-OH-PCBs as major metabolites of PCBs by rat CYP2B1 in our experiments was consistent with previous work.[32] Similar results were observed previously

in the biotransformation of dichlorobiphenyls mediated by phenobarbital-induced (i.e., CYP2B enriched) CYPs in rat liver microsomes.[33] Waller et al.[32] found that rat CYP2B1 generated 5-136 as the major metabolite of PCB 136. However, the yield rank order of 5-OH-PCB metabolites in previous rat liver microsomal studies (i.e., PCB 91 at 20% yield, PCB 95 at 8.8%, PCB 132 at 16%, PCB 136 at 22% and PCB 149 at 2.6%)[8, 24] differed somewhat from that of the present work (i.e., PCB 136 at 19%, PCB 95 at 12%, PCB 132 at 5.9%, PCB 91 at 5.4%, and PCB 149 at 1.6%). The obvious differences in the yields for 5-91 and 5'-132 suggests that other CYP isoforms, other than that mediated by CYP2B1, might be involved in the formation of these metabolites in liver microsomes. The formation of NIH-shift metabolites of chiral PCBs in the rat liver microsomes, not observed in the present study, confirmed the involvement of enzymes other than rat CYP2B1. Thus, different OH-PCBs may be formed by specific metabolic pathways. Certainly, differences in incubation conditions may also contribute to the noted differences in product formation. Similar comparisons can be made with previous *in vivo* work. For instance, 5-95, 5'-132 and 5-136 were identified as the major metabolites of the corresponding parent PCBs in rats.[27,44,45] All these observations taken together indicate that CYP2B1 is a major contributor to the metabolism of chiral PCBs to 5-OH-PCBs in rats *in vivo* as well as *in vitro* regardless of the contribution of other CYP isoforms.

Atropisomer composition changes of 5-OH-PCBs were observed in the present study (Fig. 1B2), confirming for the first time that CYP2B1 produces OH-PCBs stereoselectively. Similar EFs were measured on both enantioselective columns used (Fig. 1B2). The average EFs of 5-91, 5-95, 5'-132, 5-136 and 5-149 were 0.17, 0.20, 0.85, 0.77 and 0.41, respectively. Although the biotransformation of PCB 149 by rat CYP2B1 was not a stereoselective process, atropisomer composition change of 5-149 was indeed observed. This might be due to the stereoselective depletion of 5-OH-PCBs to diOH-PCBs by CYP2B1, which will be discussed in next section. Alternatively, covalent binding of OH-PCBs with CYPs is another possible explanation.[10, 31] It was not possible to measure the EFs of 4-OH-PCBs in our study due to the low amounts of these metabolites; however, atropisomer composition change of 4-OH-PCB in rat CYP2B1 mediated biotransformation might exist as was observed in rat liver microsomes.[27]

Comparison of our CYP-mediated OH-PCB atropisomer composition with that from liver microsomes[8, 24] and slices[25], and *in vivo* [27] studies (Table S1) indicates that while CYP2B1 is likely a dominant isozyme for production of 5-OH-PCB metabolites, other enzymes are probably also involved. The EFs of 5-91, 5-95, 5'-132, 5-136 and 5-149 from incubations of their parent PCBs with rat liver microsomes were 0.54, 0.36, 0.30, 0.70 and 0.66, respectively.[8, 24] The EFs of 5-95 (EF=0.20) and 5-136 (EF=0.77) in our CYP2B1-mediated incubations are similar, indicating that CYP2B1 plays an important role in stereoselective formation of these OH-PCBs. However, accumulation of the antipodes of 5'-132 and 5-149 implies that other biotransformation processes (e.g., biotransformation of chiral PCBs or 5-OH-PCBs by other enzymes) might be involved in the stereoselective accumulation of these metabolites in rat liver microsomes. Little is known about the atropisomer composition of OH-PCBs *in vivo*. Kania-Korwel et al.,[27] observed non-racemic 5-136 (EF≈0.4) in the livers of Sprague-Dawley rats after intraperitoneal injection of PCB 136, which contrasts with the atropisomer composition pattern of 5-136 observed in rat liver microsomes (EF=0.70) and our rat CYP2B1 incubation (EF=0.77). In female C57Bl/6 mice, the EFs of 4-95 and 5-95 in the liver were about 0.20 and 0.65 respectively.[26] Thus, biotransformation by other CYP isoforms, sulfation, glucuronidation, the formation of methylsulfones via the mercapturic acid pathway, and other factors, such as exposure pathways,[46] should be considered for fully understanding the atropisomer composition of OH-PCBs. The atropisomer compositions of OH-PCBs in wild animals are unknown and should be investigated in future studies.

4,5-DiOH-PCBs were formed as minor metabolites of PCBs 91 and 136 by rat CYP2B1 in the present study (Fig.1B1). Enantioselective analyses of these diOH-PCBs were not performed because of their low concentrations. Similar diOH-PCB metabolites were observed previously in rat and mice.[8, 24] For instance, 4,5-136 and 4,5-91 were observed in rat liver microsomes as minor metabolites.[8, 24] 4,5-136 was also found in rat livers after intraperitoneal injection of PCB 136.[27] 4',5'-132 was detected in rat liver microsomes previously,[8] which is different from our observation. Our study may not have produced enough 4',5'-132 to allow detection by our GC methods, or alternatively some other CYP isoforms might be responsible for generation of 4',5'-132 in the rat liver microsomes. 4,5-95 was found in the mice body after 39 days oral exposure.[26] DiOH-PCBs were also found in other species such as laboratory-exposed Guun rats [28] (i.e., 3',4'-dihydroxy-PCB 101) and fishes collected from Great Lakes (i.e., 4, 4'-dihydroxy-PCB 202).[29] Regardless, our study shows that hydroxylation of OH-PCBs by CYPs is a source of diOH-PCBs in biota, as noted below.

Stereoselective biotransformation of OH-PCBs and formation of diOH-PCBs

To demonstrate that OH-PCBs can be stereoselectively biotransformed by CYPs and generate non-racemic diOH-PCBs, 4-95 and 5-95 were used as model compounds. Both OH-PCBs were biotransformed by rat CYP2B1 with 40% and 64% depletion after 60 min and with the 5-95 having a significantly greater biotransformation activity (Fig.2A1). Atropisomer composition change of both substrates was found, with EFs of 0.62 and 0.46 for 4-95 and 5-95, respectively. Thus, rat CYP2B1 could metabolize OH-PCBs stereoselectively. It also suggests that OH-PCBs are potential competitors for the biotransformation of parent PCBs since they were present in the biotransformation process at the same time and both of them can be metabolized by CYP2B1. The higher concentration of E2 5-95 in the incubation of PCB 95 with CYP2B1 (EF~0.20, Fig.1B2) was consistent with the incubation using 5-95 as substrate (EF~0.46, Fig.2A2). This means that both the stereoselective biotransformation of parent PCBs and OH-PCBs contribute to the atropisomer composition change of OH-PCBs observed in biological systems.

The metabolite observed was identified as 4,5-95 for both substrates (Fig.2B1, Fig.S2A and Fig.S2B). The average yields of 4,5-95, expressed as the percent of 4,5-95 over the initial concentration of the appropriate OH-PCB, were 17% and 29% for 4-95 and 5-95, respectively. The incubation of 5-95 with rat CYP2B1 produced a significantly greater amount of 4,5-95 than the incubation of 4-95, consistent with the higher biotransformation rate of 5-95. Of the depleted OH-PCB congeners, 42% and 45% were biotransformed to 4,5-95 respectively. This result suggested that some unidentified metabolites or intermediates might have been produced. This was consistent with the unknown peaks detected in the chromatograms (Fig. S2A). The formation of 4,5-95 was also a stereoselective process, with measured EFs of 0.53 and 0.58 for 4-95 and 5-95 incubations, respectively. The atropisomer composition data of chiral diOH-PCBs in organisms are rare. Only one study demonstrated that non-racemic 4,5-95 was detected as the metabolite of PCB 95 in mice.[26] Thus, future studies are necessary to identify the atropisomer enrichment of diOH-PCBs in wildlife.

Interference between the two atropisomers of PCB 136

To understand better the mutual interference between enantiomers of chiral contaminants, individual atropisomers of PCB 136 were isolated and used in the biotransformation experiment as a model. Previous achiral work[47] on PCB 136 biotransformation by human liver microsomes (280 pmole CYP/mg protein) suggested that the V_{max} and K_m values were about 5 pmole PCB 136/mg protein/min (1.8 ng PCB 136/mg protein/min) and 8.8 μM (3200 ng/mL), respectively. In contrast, the highest substrate concentration and

biotransformation activity in the present study (90 pmole CYP/mg protein) were about 3 μM (1000 ng/mL) and 96 pmole PCB 136/mg protein/min (35ng PCB136/mg protein/min), respectively. These results indicated that the biotransformation activity of chiral PCBs by rat CYP2B1 are faster than that mediated by human CYPs, which was consistent with previous observation.[7] Certainly, different incubation conditions[47] was another possible factor contributing to the differences.

The biotransformation activity of the (−)-PCB 136 atropisomer significantly decreased with increases in initial (+)-PCB 136 concentration (Fig. 3A1), indicating that the (+)-atropisomer disrupted the biotransformation rate of the (−)-atropisomer. Correspondingly, the formation of 4-136 and 4,5-136 metabolites were also significantly decreased with increases in the initial (+)-PCB 136 concentration, which suggested that (−)-PCB 136 was the major source of these two metabolites (Fig.4A1). While the formation of 5-136 was not influenced by adding more (+)-PCB 136 as competitor, the atropisomer composition of 5-136 was changed. In the pure (−)-PCB 136 incubations, E1-5-136 was the only metabolite (Fig.4A2). Increases in the initial (+)-PCB 136 concentration resulted in significant decreases in formation of E1-5-136 and increases in E2-5-136 (ANOVA, $p<0.0001$), again consistent with the disruption of (−)-PCB 136 metabolism by (+)-PCB 136 (Fig.4A2).

Conversely, the biotransformation activity of (+)-PCB 136 was not significantly affected by the presence of (−)-PCB 136 (Fig. 3B1). The concentration of 4-136 and 4,5-136 in these incubations were lower than the incubations which use (−)-PCB 136 as the major substrate (Fig. 4A1 and 4B1). In addition, a significant increase in 4-136 formation with increases in initial (−)-PCB 136 concentration was observed (Fig. 4B1). These results were consistent with the observations above, which suggested that (−)-PCB 136 was the major source of 4-136 and 4,5-136. A significant decrease in E2-5-136 formation was indeed observed (Fig. 4B2) in these incubations. However, the decrease trend was not as significant as the decrease of E1-5-136 in Fig.4B1. These results suggest that disruption in product formation of (+)-PCB 136 metabolism by (−)-PCB 136 existed, but not as much as that of the disruption of (−)-PCB 136 by (+)-PCB 136.

Previously, Lu and Wong found that the two atropisomers of PCB 132 could disrupt the biotransformation process of each other *in vitro*.[9] One possible mechanism was that (−)-PCB 132 could “inhibit” the metabolism of (+)-PCB 132 because of higher binding affinities of (−)-PCB 132 with rat CYP2B1. However, the “inhibition” of biotransformation activity of (−)-PCB 132 from (+)-PCB 132 could not be ruled out due to unavoidable impurities of the (−)-PCB 132 in that experiment.[9] Similarly, two atropisomers of PCB 136 could bind with rat and mouse liver microsomal CYPs in a different manner.[11] In the present study, we show that the accumulation of one atropisomer of chiral PCBs (e.g., (−)-PCB 136 or (+)-PCB 132) in the biotransformation by CYPs was because its antipode (e.g., (+)-PCB 136 or (−)-PCB 132), or by extension to other chemicals, were “better” substrates of the enzymes.

In addition, the biotransformation activity of the “competitor/inhibitor” increased to a different extent with increases in its initial concentration, compared to that of its antipode (Fig. 3A2 and 3B2). It is possible that the reason why we did not see any further decreases in the biotransformation activity of (−)-PCB 136 above 250 ng/mL of (+)-PCB 136 (Fig. 3A1) is because the enzyme was saturated, as suggested in Fig. 3B2. Despite the good linear regression found, the activity may have leveled off between 250 and 500 ng/mL of (−)-PCB 136.

Environmental implications

The present study demonstrated that CYP2B1-mediated biotransformation plays important roles in the atropisomer composition change of chiral PCBs and their hydroxylated metabolites in rats. The stereoselective metabolism of racemic OH-PCBs to non-racemic diOH-PCBs by rat CYP2B1 was confirmed as a mechanism for the atropisomer composition change of the chiral OH-PCBs. These findings indicated that the stereoselective biotransformation of chiral PCBs and OH-PCBs by CYPs are major sources of non-racemic PCBs, OH-PCBs and diOH-PCBs in the environment. The disruption of both biotransformation and the product formation of chiral compounds at the enantiomer level were confirmed by the present study. Our findings help explain the underlying processes for enantiomer composition change of chiral organic contaminants observed *in vivo* and *in vitro*. There were some unidentified metabolites in the biotransformation of chiral PCBs and OH-PCBs by rat CYP2B1, which may suggest potential exposure to these metabolites in the environment warranting further investigation.

Supplementary Material

Refer to Web version on PubMed Central for supplementary material.

Acknowledgments

Funding was provided by grant ES017425 from the National Institute of Environmental Health Sciences, National Institutes of Health (to HJL and IKK), the Natural Sciences and Engineering Research Council of Canada, the Canada Research Chairs Program (to CSW); and a Chinese Government Award for Outstanding Self-Financed Students Abroad from the China Scholarship Council (to ZL). We also acknowledge support through the Environmental Health Sciences Center (NIEHS/NIH grant P30 ES05605) and the Superfund Research Program (NIEHS/NIH grant P42 ES013661) at The University of Iowa. We thank Jennifer Low for helpful technical assistance.

Literature cited

1. Lehmler H-J, Harrad SJ, Hühnerfuss H, Kania-Korwel I, Lee CM, Lu Z, Wong CS. Chiral polychlorinated biphenyl transport, metabolism, and distribution: a review. Environ. Sci. Technol. 2010; 44:2757–2766. [PubMed: 20384371]
2. Zhai G, Hu D, Lehmler H-J, Schnoor JL. Enantioselective biotransformation of chiral PCBs in whole poplar plants. Environ. Sci. Technol. 2011; 45:2308–2316. [PubMed: 21329345]
3. Wayman GA, Bose DD, Yang D, Lesiak A, Bruun D, Impey S, Ledoux V, Pessah IN, Lein PJ. PCB-95 modulates the calcium-dependent signaling pathway responsible for activity-dependent dendritic growth. Environ. Health Perspect. 2012; 120:1003–1009. [PubMed: 22534176]
4. Pessah IN, Hansen LG, Albertson TE, Garner CE, Ta TA, Do Z, Kim KH, Wong PW. Structure-activity relationship for noncoplanar polychlorinated biphenyl congeners toward the ryanodine receptor-Ca^{2+} channel complex type 1 (RyR1). Chem. Res. Toxicol. 2006; 19:92–101. [PubMed: 16411661]
5. Mariussen E, Fonnum F. Neurochemical targets and behavioral effects of organohalogen compounds: An update. Crit. Rev. Toxicol. 2006; 36:253–289. [PubMed: 16686424]
6. Pessah IN, Lehmler H-J, Robertson LW, Perez CF, Cabrales E, Bose DD, Feng W. Enantiomeric specificity of (−)-2,2′,3,3′,6,6′-hexachlorobiphenyl toward Ryanodine receptor types 1 and 2. Chem. Res. Toxicol. 2009; 22:201–207. [PubMed: 18954145]
7. Warner NA, Martin JW, Wong CS. Chiral polychlorinated biphenyls are biotransformed enantioselectively by mammalian cytochrome P-450 isozymes to form hydroxylated metabolites. Environ. Sci. Technol. 2009; 43:114–121. [PubMed: 19209593]
8. Kania-Korwel I, Duffel MW, Lehmler H-J. Gas chromatographic analysis with chiral cyclodextrin phases reveals the enantioselective formation of hydroxylated polychlorinated biphenyls by rat liver microsomes. Environ. Sci. Technol. 2011; 45:9590–9596. [PubMed: 21966948]

9. Lu Z, Wong CS. Factors affecting Phase I stereoselective biotransformation of chiral polychlorinated biphenyls by rat cytochrome P-450 2B1 isozyme. Environ. Sci. Technol. 2011; 45:8298–8305. [PubMed: 21863805]
10. Letcher R, Klasson-Wehler E, Bergman Å . Methyl sulfone and hydroxylated metabolites of polychlorinated biphenyls. Handbook of Environmental Chemistry. 2000; 3K:315–359.
11. Kania-Korwel I, Hrycay EG, Bandiera SM, Lehmler H-J. 2,2′,3,3′,6,6′-Hexachlorobiphenyl (PCB 136) atropisomers interact enantioselectively with hepatic microsomal cytochrome P450 enzymes. Chem. Res. Toxicol. 2008; 21:1295–1303. [PubMed: 18494506]
12. Buckman AH, Wong CS, Chow EA, Brown SB, Solomon KR, Fisk AT. Biotransformation of polychlorinated biphenyls (PCBs) and bioformation of hydroxylated PCBs in fish. Aquat. Toxicol. 2006; 78:176–185. [PubMed: 16621064]
13. Richardson KL, Schlenk D. Biotransformation of 2,2′,5,5′-tetrachlorobiphenyl (PCB 52) and 3,3′, 4,4′-tetrachlorobiphenyl (PCB 77) by liver microsomes from four species of sea turtles. Chem. Res. Toxicol. 2011; 24:718–725. [PubMed: 21480586]
14. Jörundsdóttir H, Löfstrand K, Svavarsson J, Bignert A, Bergman Å. Organochlorine compounds and their metabolites in seven Icelandic seabird species - a comparative study. Environ. Sci. Technol. 2010; 44:3252–3259. [PubMed: 20356092]
15. Weijs L, Das K, Siebert U, van Elk N, Jauniaux T, Neels H, Blust R, Covaci A. Concentrations of chlorinated and brominated contaminants and their metabolites in serum of harbour seals and harbour porpoises. Environ. Int. 2009; 35:842–850. [PubMed: 19303641]
16. McKinney MA, De Guise S, Martineau D, Béland P, Lebeuf M, Letcher RJ. Organohalogen contaminants and metabolites in beluga whale (Delphinapterus leucas) liver from two Canadian populations. Environ. Toxicol. Chem. 2006; 25:1246–1257. [PubMed: 16704055]
17. Routti H, Letcher RJ, Arukwe A, Bavel B, Yoccoz NG, Chu S, Gabrielsen GW. Biotransformation of PCBs in relation to Phase I and II xenobiotic-metabolizing enzyme activities in Ringed Seals (Phoca hispida) from Svalbard and the Baltic Sea. Environ. Sci. Technol. 2008; 42:8952–8958. [PubMed: 19192824]
18. Sandala G, Sonne-Hansen C, Dietz R, Muir D, Valters K, Bennett E, Born E, Letcher R. Hydroxylated and methyl sulfone PCB metabolites in adipose and whole blood of polar bear (Ursus maritimus) from East Greenland. Sci. Total Environ. 2004; 331:125–141. [PubMed: 15325145]
19. Gómara B, Athanasiadou M, Quintanilla-López JE, González MJ, Bergman Å. Polychlorinated biphenyls and their hydroxylated metabolites in placenta from Madrid mothers. Environ. Sci. Pollut. Res. 2012; 19:139–147.
20. Berghe MV, Weijs L, Habran S, Das K, Bugli C, Pillet S, Rees JF, Pomeroy P, Covaci A, Debier C. Effects of polychlorobiphenyls, polybromodiphenylethers, organochlorine pesticides and their metabolites on vitamin A status in lactating grey seals. Environ. Res. 2013; 120:18–26. [PubMed: 23051620]
21. Kimura-Kuroda J, Nagata I, Kuroda Y. Disrupting effects of hydroxy-polychlorinated biphenyl (PCB) congeners on neuronal development of cerebellar Purkinje cells: a possible causal factor for developmental brain disorders? Chemosphere. 2007; 67:S412–S420. [PubMed: 17223178]
22. Dreiem A, Rykken S, Lehmler H-J, Robertson LW, Fonnum F. Hydroxylated polychlorinated biphenyls increase reactive oxygen species formation and induce cell death in cultured cerebellar granule cells. Toxicol. Appl. Pharm. 2009; 240:306–313.
23. Mortensen AS, Braathen M, Sandvik M, Arukwe A. Effects of hydroxy-polychlorinated biphenyl (OH-PCB) congeners on the xenobiotic biotransformation gene expression patterns in primary culture of Atlantic salmon (*Salmo salar*) hepatocytes. Ecotox. Environ. Safe. 2007; 68:351–360.
24. Wu X, Pramanik A, Duffel MW, Hrycay EG, Bandiera SM, Lehmler H-J, Kania-Korwel I. 2, 2′, 3, 3′, 6, 6′-Hexachlorobiphenyl (PCB 136) is enantioselectively oxidized to hydroxylated metabolites by rat liver microsomes. Chem. Res. Toxicol. 2011; 24:2249–2257. [PubMed: 22026639]
25. Wu X, Kania-Korwel I, Chen H, Stamou M, Dammanahalli KJ, Duffel M, Lein PJ, Lehmler H-J. Metabolism of 2,2',3,3',6,6'-hexachlorobiphenyl (PCB 136) atropisomers in tissue slices from phenobarbital or dexamethasone-induced rats is sex-dependent. Xenobiotica. 2013 in press DOI: 10.3109/00498254.2013.785626.

26. Kania-Korwel I, Barnhart CD, Stamou M, Truong KM, El-Komy MH, Lein PJ, Veng-Pedersen P, Lehmler H-J. 2,2′,3,5′,6-pentachlorobiphenyl (PCB 95) and its hydroxylated metabolites are enantiomerically enriched in female mice. Environ. Sci. Technol. 2012; 46:11393–11401. [PubMed: 22974126]
27. Kania-Korwel I, Vyas SM, Song Y, Lehmler H-J. Gas chromatographic separation of methoxylated polychlorinated biphenyl atropisomers. J. Chromatogr. A. 2008; 1207:146–154. [PubMed: 18760792]
28. Haraguchi K, Kato Y, Koga N, Degawa M. Metabolism of polychlorinated biphenyls by Gunn Rats: Identification and serum retention of catechol metabolites. Chem. Res. Toxicol. 2004; 17:1684–1691. [PubMed: 15606145]
29. Campbell LM, Muir DCG, Whittle DM, Backus S, Norstrom RJ, Fisk AT. Hydroxylated PCBs and other chlorinated phenolic compounds in lake trout (Salvelinus namaycush) blood plasma from the Great Lakes region. Environ. Sci. Technol. 2003; 37:1720–1725. [PubMed: 12775040]
30. Nomiyama K, Uchiyama Y, Horiuchi S, Eguchi A, Mizukawa H, Hirata SH, Shinohara R, Tanabe S. Organohalogen compounds and their metabolites in the blood of Japanese amberjack (*Seriola quinqueradiata*) and scalloped hammerhead shark (*Sphyrna lewini*) from Japanese coastal waters. Chemosphere. 2011; 85:315–321. [PubMed: 21782210]
31. McLean MR, Bauer U, Amaro AR, Robertson LW. Identification of catechol and hydroquinone metabolites of 4-monochlorobiphenyl. Chem. Res. Toxicol. 1996; 9:158–164. [PubMed: 8924585]
32. Waller SC, He YA, Harlow GR, He YQ, Mash EA, Halpert JR. 2,2',3,3',6,6'-hexachlorobiphenyl hydroxylation by active site mutants of cytochrome P450 2B1 and 2B11. Chem. Res. Toxicol. 1999; 12:690–699. [PubMed: 10458702]
33. Kaminsky LS, Kennedy MW, Adams SM, Guengerich FP. Metabolism of dichlorobiphenyls by highly purified isozymes of rat liver cytochrome P-450. Biochemistry. 1981; 20:7379–7384. [PubMed: 6798990]
34. Asher BJ, D'Agostino LA, Way JD, Wong CS, Harynuk JJ. Comparison of peak integration methods for the determination of enantiomeric fraction in environmental samples. Chemosphere. 2009; 75:1042–1048. [PubMed: 19215960]
35. Haglund P, Wiberg K. Determination of the gas chromatographic elution sequences of the (+)- and (−)-enantiomers of stable atropisomeric PCBs on Chirasil-Dex. J. High Resolut. Chro. Matogr. 1996; 19:373–376.
36. Wong CS, Hoekstra PF, Karlsson H, Backus SM, Mabury SA, Muir DCG. Enantiomer fractions of chiral organochlorine pesticides and polychlorinated biphenyls in Standard and Certified Reference Materials. Chemosphere. 2002; 49:1339–1347. [PubMed: 12489731]
37. Warner NA, Norstrom RJ, Wong CS, Fisk AT. Enantiomeric fractions of chiral polychlorinated biphenyls provide insights on biotransformation capacity of arctic biota. Environ. Toxicol. Chem. 2005; 24:2763–2767. [PubMed: 16398111]
38. Chu S, Covaci A, Van de Vijver K, De Coen W, Blust R, Schepens P. Enantiomeric signatures of chiral polychlorinated biphenyl atropisomers in livers of harbour porpoises (Phocoena phocoena) from the southern North Sea. J. Environ. Monitor. 2003; 5:521–526.
39. Borlakoglu JT, Wilkins JP. Correlations between the molecular structures of polyhalogenated biphenyls and their metabolism by hepatic microsomal monooxygenases. Comp. Biochem. Physiol. 1993; 105C:113–117.
40. Kania-Korwel I, Garrison AW, Avants JK, Hornbuckle KC, Robertson LW, Sulkowski WW, Lehmler H-J. Distribution of chiral PCBs in selected tissues in the laboratory Rat. Environ. Sci. Technol. 2006; 40:3704–3710. [PubMed: 16830530]
41. Norström K, Eriksson J, Haglund J, Silvari V, Bergman Å. Enantioselective formation of methyl sulfone metabolites of 2,2′,3,3′,4,6′-hexachlorobiphenyl in rat. Environ. Sci. Technol. 2006; 40:7649–7655. [PubMed: 17256508]
42. Kania-Korwel I, Hornbuckle KC, Robertson LW, Lehmler H-J. Dose-dependent enantiomeric enrichment of 2,2',3,3',6,6'-hexachlorobiphenyl in female mice. Environ. Toxicol. Chem. 2008; 27:299–305. [PubMed: 18348647]

43. Lu Z, Ma G, Veinot JGC, Wong CS. Disruption of biomolecule function by nanoparticles: How do gold nanoparticles affect phase I biotransformation of persistent organic pollutants? Chemosphere. 2013 in press DOI: 10.1016/j.chemosphere.2013.05.004.

44. Sundström G, Jansson B. The metabolism of 2,2′,3,5′,6-pentachlorobiphenyl in rats, mice and quails. Chemosphere. 1975; 4:361–370.

45. Haraguchi K, Kato Y, Koga N, Degawa M. Species differences in the tissue distribution of catechol and methylsulphonyl metabolites of 2,4,5,2',5'-penta- and 2,3,4,2',3‘,6’-hexachlorobiphenyls in rats, mice, hamsters and guinea pigs. Xenobiotica. 2005; 35:85–96. [PubMed: 15788370]

46. Kania-Korwel I, Shaikh NS, Hornbuckle KC, Robertson LW, Lehmler H-J. Enantioselective disposition of PCB 136 (2,2′,3,3′,6,6′-hexachlorobiphenyl) in C57BL/6 mice after oral and intraperitoneal administration. Chirality. 2007; 66:56–66. [PubMed: 17089340]

47. Schnellmann R, Putnam C, Sipes I. Metabolism of 2, 2’,3,’,6,’-hexachlorobiphenyl and 2,2’,4,4’, 5,5’-hexachlorobiphenyl by human hepatic microsomes. Biochem. Pharmacol. 1983; 32:3233–3239. [PubMed: 6416258]

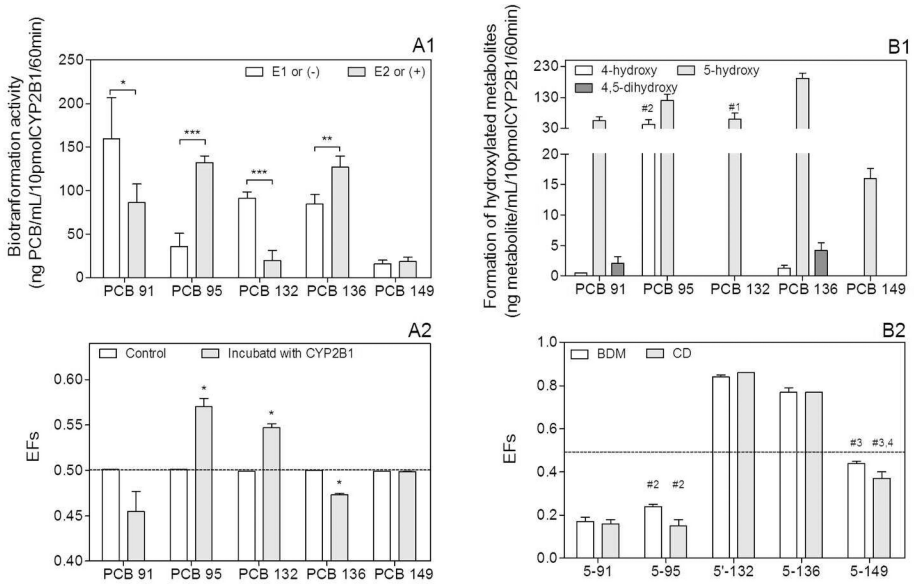

Figure 1.

Stereoselective biotransformation of chiral PCBs and formation of hydroxylated metabolites by rat CYP2B1 over 60 min incubation time, under conditions to foster generation of metabolites. (A1) Biotransformation activities of chiral PCBs (asterisks indicate statistical difference between two atropisomers of a chiral PCB, unpaired t-test, one-tailed *p* value,* $p<0.05$, ** $p<0.01$, *** $p<0.001$); (A2) Enantiomer fractions (EFs) of chiral PCBs after biotransformation (asterisks indicate statistical difference, one sample t-test, two-tailed *p* value *$p<0.05$, different from racemic i.e., 0.5); (B1) Formation activities of mono- and di-hydroxylated metabolites of PCBs; (B2) EFs of 5-hydroxy metabolites of chiral PCBs determined on two different enantioselective gas chromatography columns. All the EFs are statistically different from 0.5. CD: Chirasil-Dex column; BDM: ChiralDex B-DM column. All data reported as mean±standard deviation of three replicates (one sample for each negative control). [#1]Value not adjusted for recovery because the surrogate standard co-eluted with 4,5-132; [#2]Not detected by GC-MS; [#3]Imperfect agreement of EFs between BDM and CD column; the atropisomers of various metabolites co-eluted on both columns, making the EF determination difficult; [#4]The results were confirmed on CD column using a mass selective detector, EF = 0.31 ± 0.03. Raw data are shown in Table S2 in SI.

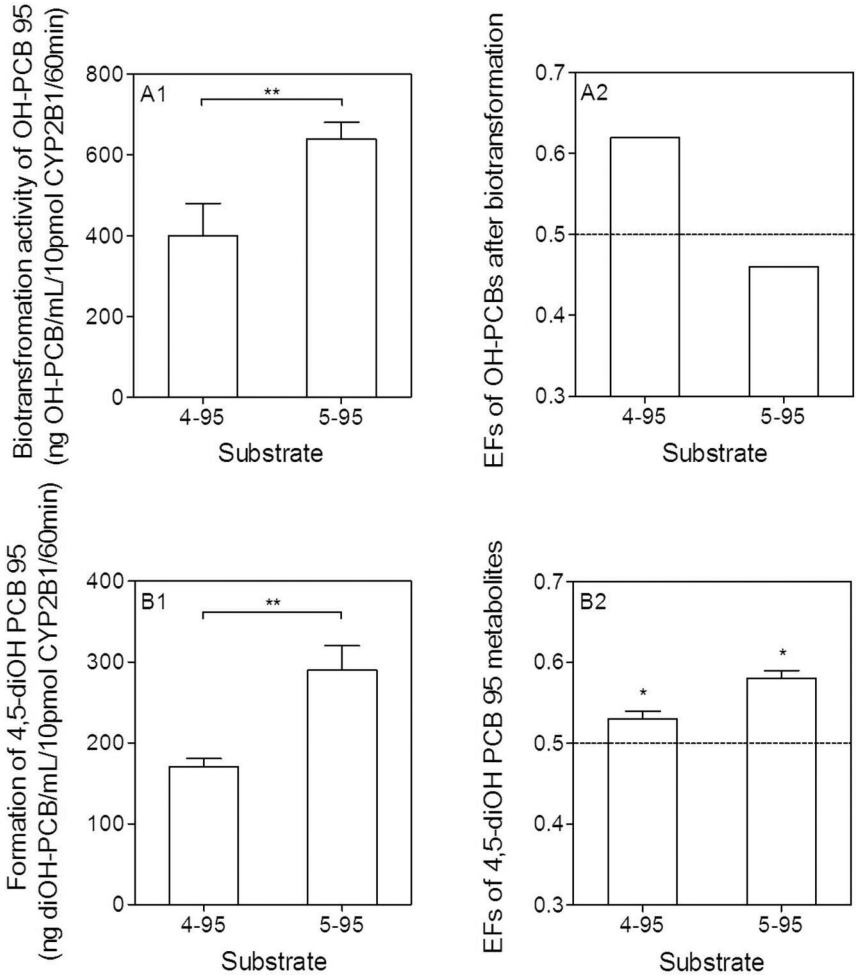

Figure 2.

Stereoselective biotransformation of 4-95 and 5-95 and formation of 4,5-95 by rat CYP2B1, over 60 min incubation time. (A1) Biotransformation activities of 4-95 and 5-95 by rat CYP2B1 (asterisks indicate statistical difference, unpaired t-test, one-tailed *p* value, * $p<0.05$, ** $p<0.01$); (A2) EFs of 4-95 and 5-95 after biotransformation; (B1) Formation activities of 4,5-95 after biotransformation of 4-95 and 5-95 by rat CYP2B1 (asterisks indicate statistical difference, unpaired t-test, one-tailed *p* value, ** $p<0.01$); (B2) EFs of 4,5-95 as metabolite of OH-PCB 95 derivatives (asterisks indicate statistical difference from racemic, i.e., 0.5). Values are presented as mean ± standard deviation of three replicates. Raw data are shown in Table S3 in SI.

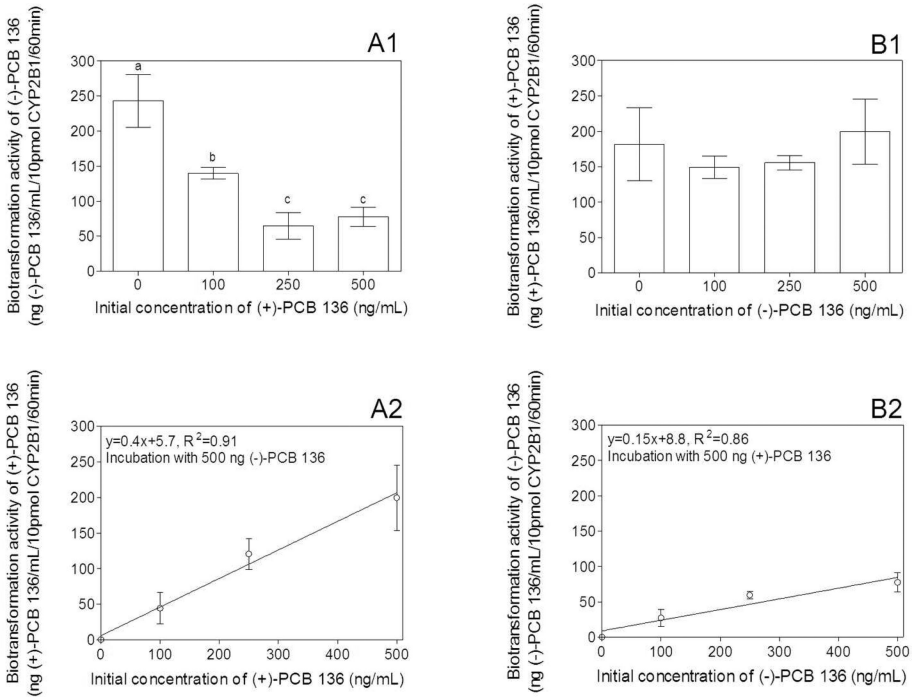

Figure 3.

The two atropisomers of PCB 136 interfere with each other when biotransformed by rat CYP2B1. (A) Incubation of 500 ng (−)-PCB 136 with various initial concentrations of (+)-PCB 136: (A1) biotransformation activities of (−)-PCB 136, (A2) biotransformation activities of (+)-PCB 136; (B) Incubation of 500 ng (+)-PCB 136 with various initial concentrations of (−)-PCB 136: (B1) biotransformation activities of (+)-PCB 136, (A2) biotransformation activities of (−)-PCB 136. All data reported as mean±standard deviation of three replicates. Different letters in A1 and B1 indicate statistical difference in biotransformation activities, $p<0.05$, one way ANOVA with post Tukey's multiple comparison test. Raw data are shown in Table S4 in SI. All incubations over 60 min.

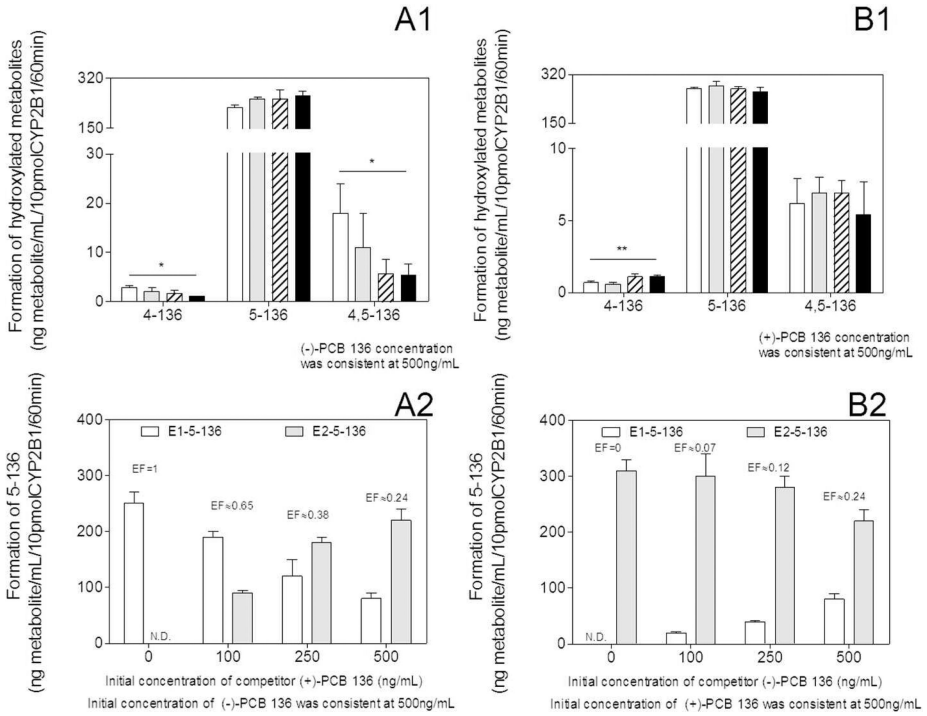

Figure 4.

The two atropisomers of PCB 136 interfere with each other when producing hydroxylated metabolites in biotransformation by rat CYP2B1. (A) Incubation of 500 ng (−)-PCB 136 with various initial concentrations of (+)-PCB 136: (A1) formation activities of 4-136, 5-136 and 4,5-136, (A2) formation activity of the two atropisomers of 5-136; (B) Incubation of 500 ng (+)-PCB 136 with various initial concentrations of (−)-PCB 136: (B1) formation activities of 4-136, 5-136 and 4,5-136, (B2) formation activities of the two atropisomers of 5-136. All data reported as mean±standard deviation of three replicates. N.D. = not detected. Asterisks in A1 and B1 indicate statistical difference, *p<0.05, **p<0.01, one way ANOVA with post Tukey's multiple comparison test. Raw data are shown in Table S4 in SI. The chromatograms of the metabolites of pure (−)-or (+)-PCB 136 by rat CYP2B1 are shown in SI (Fig. S3A and S3B). All incubations over 60 min.